A MOLECULARLY DEFINED POLYMERIC PLATFORM FOR ENVIRONMENTALLY RESPONSIVE ACTIVATION OF STING TO ENHANCE CANCER IMMUNOTHERAPY

Jacob A. Schulman [1]; Karan Arora, Ph.D. [2]; Alexander J. Kwiatkowski [2]; Neil C. Chada [1]; Hayden M. Pagendarm [1]; John T. Wilson, Ph.D. [1,2]

[1] Department of Biomedical Engineering, Vanderbilt University; [2] Department of Chemical and Biomolecular Engineering, Vanderbilt University

Introduction

The stimulator of interferon genes (STING) pathway is a promising immuno-oncology target. Despite their potential, STING agonists have yielded underwhelming results in clinical trials due to pharmacological barriers that limit their safety and efficacy. Herein, we describe the design and pre-clinical evaluation of a polymer-dimeric amidobenzimidazole (diABZI) STING agonist conjugate platform for cancer immunotherapy. Central to our technology is a stimuli-responsive diABZI-functionalized reversible addition-fragmentation chain transfer (RAFT) polymerization chain transfer agent (CTA) that allows well-defined polymer chains to be grown directly from a single STING agonist. Using a biocompatible poly(N,N'-dimethylacrylamide) polymer as a first-generation scaffold and a disulfide as a clinically relevant linker, we demonstrate that polymer-STING agonist conjugates liberate diABZI under reducing conditions to trigger STING activation in tumors, thereby stimulating antitumor immunity in multiple murine tumor models and synergizing with α-PD-1 immune checkpoint blockade to eliminate tumors. This work therefore establishes a versatile delivery platform for microenvironmental regulation of STING activation with promise as an immunotherapy for cancer.

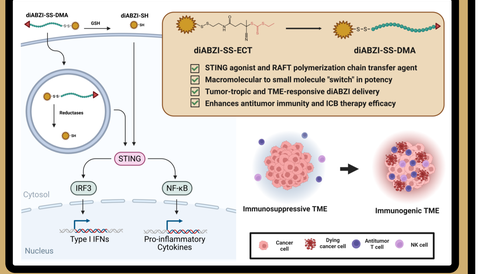

In Vivo STING Activation and Efficacy in Immunogenic Flank Tumor Model

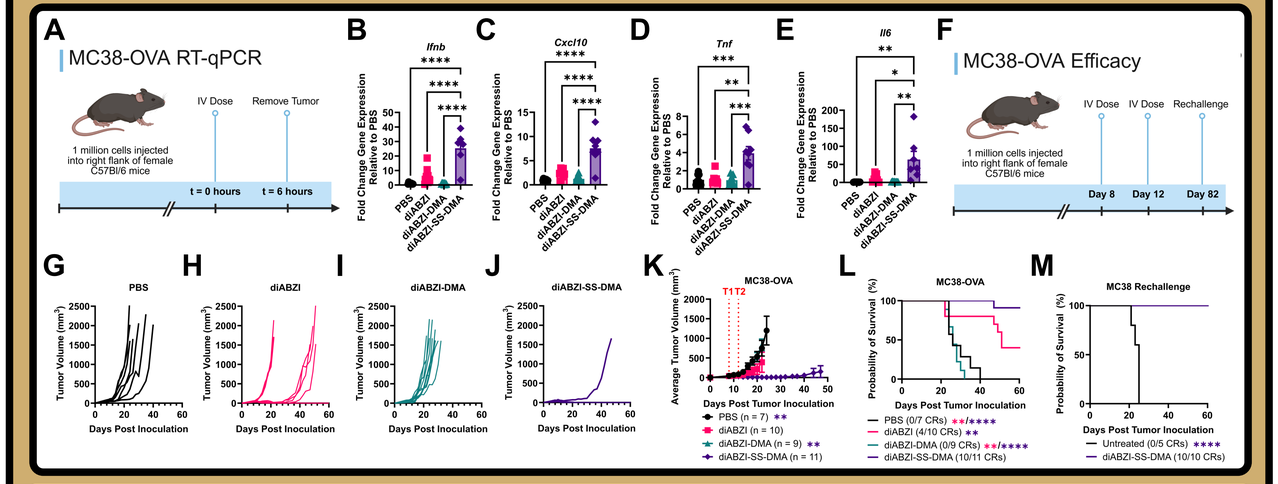

(A) Schematic of subcutaneous MC38-OVA tumor inoculation, treatment schedule, and study endpoint to quantify gene expression changes in the tumor after diABZI-SS-DMA treatment compared to PBS, diABZI, and diABZI-DMA controls. **(B to E)** Fold change of STING-associated genes, *Ifnb*, *Cxcl10*, *Tnf*, and *Il6* in response to treatment via RT-qPCR (n = 6 to 8). Gene expression was normalized to *Hmbs*, a housekeeping gene that is not impacted by STING activation, followed by normalization to PBS. **(F)** Schematic of subcutaneous MC38-OVA tumor inoculation and treatment/rechallenge schedule to quantify efficacy of diABZI-SS-DMA treatment compared to PBS, diABZI, and diABZI-DMA controls. **(G to J)** Spider plots of individual tumor growth curves for each treatment group. **(K)** Average tumor volume until 1st death in each treatment group. **(L)** Kaplan-Meier survival plots for treatment groups. Statistical comparisons for tumor burden were evaluated at the time of first death, regardless of experimental group, using the total area under the curve from day 0 to the day of first mouse death (mm^3·days). **(M)** Kaplan–Meier survival plots for MC38 tumor rechallenge in untreated (i.e., naïve) or complete responders (CRs) from diABZI-SS-DMA treatment.

In Vitro Characterization of Polymeric diABZI Prodrug, diABZI-SS-DMA

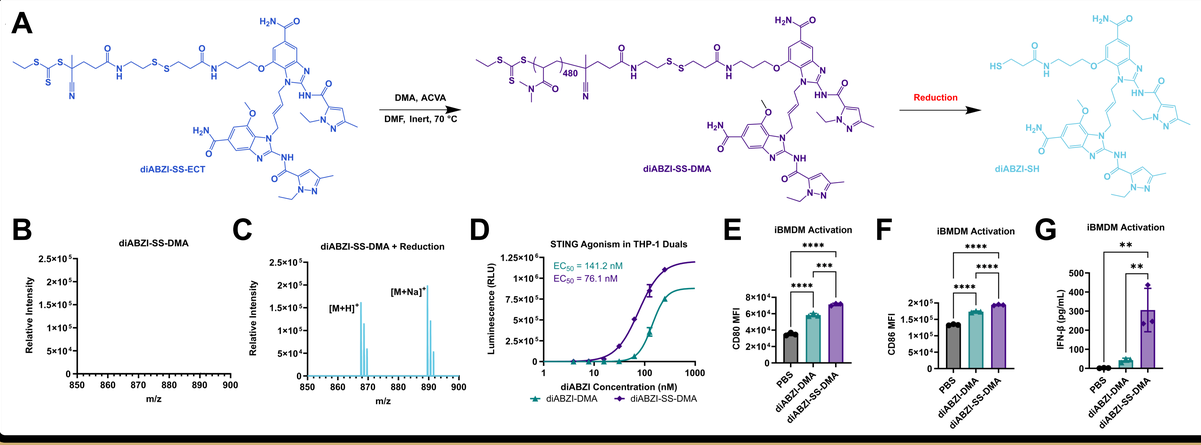

(A) Scheme for synthesis of polymeric prodrug diABZI-SS-DMA and reduction-responsive release of potent STING agonist, diABZI-SH. **(B to C)** MALDI-MS spectra for diABZI-SS-DMA, and diABZI-SS-DMA + Reduction conditions, demonstrating reduction-responsive diABZI-SH release from diABZI-SS-DMA. **(D)** Dose-dependent STING agonism in THP-1 Dual reporter cells after 24-hour treatment with diABZI-SS-DMA or diABZI-DMA at indicated concentrations via QUANTILuc assay, a measure of relative IRF3 signaling (n = 3). **(E to F)** Mean fluorescence intensity (MFI) of surface activation markers, CD80 and CD86, in immortalized bone marrow-derived macrophages (iBMDMs) after 24-hour treatment with diABZI-SS-DMA, diABZI-DMA, or PBS at 500 nM diABZI concentration via flow cytometry (n = 3). **(G)** Secreted IFN-β in iBMDM supernatant after 24-hour treatment with diABZI-SS-DMA, diABZI-DMA, or PBS at 500 nM diABZI concentration via sandwich ELISA (n = 3).

In Vivo Biodistribution in Immunogenic Flank Tumor Model

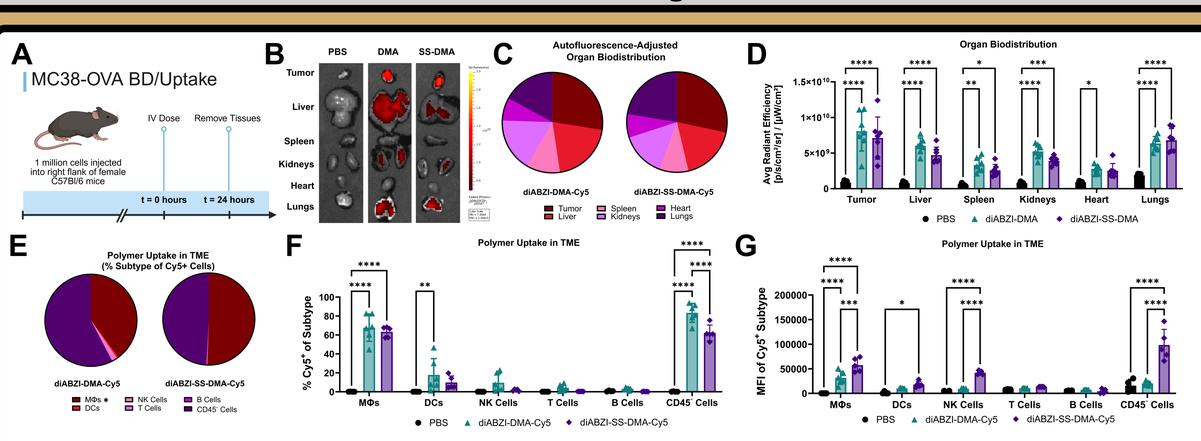

(A) Schematic of subcutaneous MC38-OVA tumor inoculation, treatment schedule, and study endpoint to quantify diABZI-SS-DMA-Cy5 and diABZI-DMA-Cy5 organ biodistribution and cellular uptake in the TME compared to PBS control. **(B)** Representative IVIS images of excised tissue 24 hours following systemic administration. **(C)** Percentage of Cy5 fluorescence in each tissue after adjusting for organ-specific autofluorescence (n = 5 to 6). **(D)** Average radiant efficiency of Cy5 in each tissue (n = 5 to 6). **(E)** Percentage of Cy5⁺ cells by subtype out of all Cy5⁺ cells in tumor (n = 5 to 6). **(F)** Percentage of Cy5⁺ cells within given subtype in tumor (n = 5 to 6). **(G)** Mean fluorescence intensity (MFI) of Cy5 in Cy5⁺ subtype (n = 5 to 6).

In Vivo Efficacy in Immunosuppressive Orthotopic Tumor Model

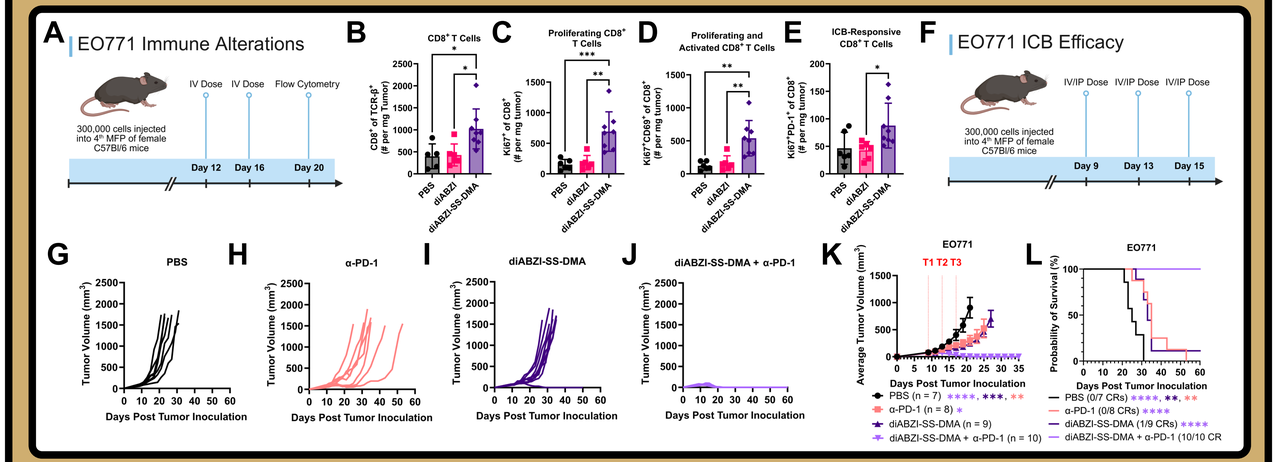

(A) Schematic of orthotopic EO771 tumor inoculation and treatment/flow cytometry schedule to quantify efficacy of diABZI-SS-DMA treatment compared to PBS and diABZI controls. **(B to D)** Absolute number of CD8+ T cells and proliferating (Ki67⁺) and proliferating, activated (Ki67⁺CD69⁺) CD8+ T cells per mg tumor. **(E)** Absolute number of α-PD-1 ICB-responsive (Ki67⁺PD-1⁺) CD8+ T cells per mg tumor **(F)** Schematic of orthotopic EO771 tumor inoculation and treatment schedule to quantify efficacy of diABZI-SS-DMA and α-PD-1 ICB treatment compared to PBS, α-PD-1, and diABZI-SS-DMA controls. **(G to J)** Spider plots of individual tumor growth curves for each treatment group. **(K)** Average tumor volume until 1st death in each treatment group. Statistical comparisons for tumor burden were evaluated at the time of first death using the total area under the curve over the entire study (mm^3·days). **(L)** Kaplan-Meier survival plots for treatment groups.

Conclusions/Acknowledgements

We describe the design, synthesis, and pre-clinical evaluation of a next-generation polymeric STING agonist carrier, diABZI-SS-DMA to improve the pharmacological profile and antitumor efficacy of diABZI. Despite lacking any tumor- or cell-targeting functionalities, diABZI-SS-DMA preferentially delivers diABZI to the tumor, exhibits high tumor-associated macrophage uptake, and significantly increases STING-related gene expression within the TME. Accordingly, diABZI-SS-DMA monotherapy significantly reduces tumor burden and enhances survival in multiple tumor models, outperforming leading STING agonist, diABZI. Moreover, diABZI-SS-DMA potentiates α-PD-1 therapy in an immunotherapy-unresponsive, orthotopic triple-negative breast cancer model. Collectively, this work establishes diABZI-functionalized RAFT polymerization chain transfer agents as a promising and enabling platform for engineering of next-generation polymeric carriers for the systemic delivery of STING agonists to eradicate solid tumors and synergize with ICB therapy.

NSF
NIH
National Institutes of Health
GRFP